Inelastic collisions of ultracold polar molecules

John L. Bohn*
JILA, National Institute of Standards and Technology and University of Colorado, Boulder, Colorado 80309-0440
(Received 7 August 2000; published 17 April 2001)

The collisional stability of ultracold polar molecules in electrostatic traps is considered. Rate constants for collisions that drive molecules from weak-electric-field-seeking to strong-field-seeking states are estimated using a simple model that emphasizes long-range dipolar forces. The rate constants for collisional losses are found to vary substantially as a function of molecular parameters used in the model, such as dipole moment, mass, and the splitting of the molecular Λ doublet. Varying these parameters over physically reasonable ranges yields rate constants as low as 10^{-20} cm^3/sec and as high as 10^{-10} cm^3/sec. Nevertheless, the loss rates rise dramatically in the presence of the externally applied trapping electric field. For this reason it is argued that electrostatic traps are likely to be less stable against collisional losses than their magnetic counterparts.

DOI: 10.1103/PhysRevA.63.052714 PACS number(s): 34.50.−s, 34.50.Ez

Recently Bethlem *et al.* broadened the scope of ultracold molecular physics by cooling and electrostatically trapping ND_3 molecules [1,2]. This achievement is notable both for the complexity of the species trapped and for the generality of the Stark slowing technique, which could in principle cool any polar molecule. This technique is therefore now on a par with other experimental methods for producing cold molecular gases, such as photoassociation [3] and buffer-gas cooling [4], as well as photoproduction of molecular ions in a Paul trap [5].

The electrostatic trap demonstrated in Ref. [2] raises anew questions of collisional stability that are familiar in the context of magnetic trapping of atoms [6]. An electrostatic trap can only confine dipoles that are in their weak-field-seeking states, since Maxwell's equations permit a local field minimum but not a field maximum. Thus the dipoles are susceptible to orientation-changing collisions that populate the strong-field-seeking, untrapped states. In the case of magnetic trapping of alkali-metal atoms a standard remedy against collisional losses is to prepare the atoms in their stretched spin states, whereby the dominant spin-exchange collisional processes are absent. Atomic spins can then change their orientation only via spin-spin dipolar processes, which are weak because of the inherent weakness of magnetic dipolar interactions.

The purpose of this paper is to point out that polar molecules are not as immune to dipolar relaxation as are magnetic atoms, simply because electric dipoles have a much stronger interaction. Indeed, the force between a pair of $d=1$ D (0.39 a.u.) electric dipoles is $\sim 3\times 10^3$ times larger than that between a pair of $\mu = 1\mu_B$ magnetic dipoles. The basic physics of electric dipolar relaxation lies in the competition between the dipoles' interaction with the electric field when they are far apart, $-\vec{d}\cdot\vec{\mathcal{E}}$, and with each other when they are closer together, $\sim \vec{d}_1\cdot\vec{d}_2/R^3$. At small values of intermolecular separation R the dipoles will tend to lock on their intermolecular axis rather than on the laboratory-fixed axis set by $\vec{\mathcal{E}}$; the competition between these tendencies scrambles the orientation of the molecular dipoles. The resulting state-changing collisions can in principle be suppressed by a field strong enough to maintain the dipolar orientation. This will happen, roughly, if $d\mathcal{E} > d^2/R^3$ for small values of R. Still, for $d=1$ D dipoles at a typical collision distance $R\approx 10$ a.u., an electric field of 10^6 V/cm would be required to maintain dipolar orientation. Thus very large laboratory fields may exert some mitigating influence, but are unlikely to arrest relaxation altogether.

To quantify this general argument this paper presents detailed calculations using a simplified model of collisions. In general the physics of cold molecular collisions will be quite complex, intertwining rotational, electronic, nuclear spin, and perhaps even vibrational degrees of freedom. However, to establish orders of magnitude for dipolar relaxation rate constants it suffices to focus on orientational degrees of freedom, and to account only for the dominant dipole-dipole interaction between molecules. Accordingly, a simplified ''toy'' model is used here, which has zero spin and nuclear spin. The molecules are assumed to be diatomic rigid rotors with electric dipole moments d along their molecular axes. The electronic ground state of the molecule is assumed to be $^1\Pi$, so that it possesses a Λ doublet of parity eigenstates with splitting $\Delta = q_\Lambda N(N+1)$, where q_Λ is the Λ doublet parameter and N is the molecule's rotational quantum number. In the model used here we will generally assume that the lower state of the Λ doublet has even parity $p=+1$.

At ultracold temperatures and in zero electric field the molecules occupy parity eigenstates, and hence exhibit no permanent dipole moment. The dipole moments become apparent only when the field is large enough to significantly mix states of different parity, thus ''activating'' the dipoles. This occurs at a field value where the Stark effect transforms from quadratic to linear at a field value $\mathcal{E}_0 \approx \Delta/d$ (Fig. 1). For fields below this value the molecules are fairly weakly interacting, whereas above this value the molecules have extremely strong dipole couplings. Thus in a state with Λ doubling collisions can be manipulated using modest electric fields, in contrast to the $\sim 10^5$ V/cm fields required to influence cold atomic collisions [7]. These arguments also apply to molecules with $^{2S+1}\Sigma$ electronic symmetry when $S>0$ and the molecule exhibits an Ω doubling [8], as well as to ND_3.

*Electronic address: bohn@murphy.colorado.edu

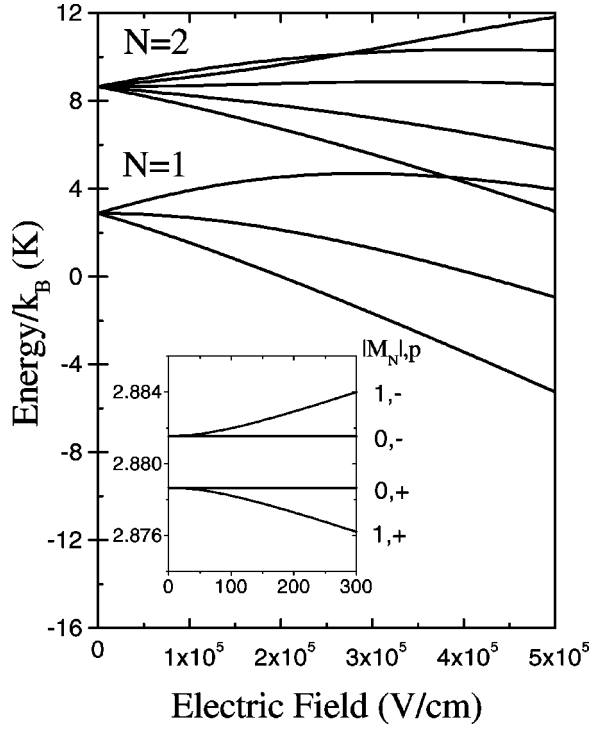

FIG. 1. Stark energy levels for the model molecules, which have $^1\Pi$ electronic symmetry. Shown is the case $d=1$ D, $q_\Lambda = 10^{-3}$ cm^{-1}. This paper concentrates on collisions between molecules in their $|M_N,p\rangle = |+1,-\rangle$ states, which are weak-field seekers (see inset).

Figure 1 shows the electric-field dependence of the lowest-lying energy levels in the model molecules, for the particular values $d=1$ D and $q_\Lambda = 10^{-3}$ cm^{-1}. Although both $N=1$ and $N=2$ rotational levels are shown, the calculations below focus exclusively on the $N=1$ levels. Their low-$\mathcal{E}$ behavior is shown in the inset, labeled by the pair of quantum numbers $|M_N|,p$. Here p stands for the parity in zero field, while $|M_N|$ denotes the magnitude of the molecular rotation's magnetic quantum number referred to the laboratory axis; the $M_N=1$ and $M_N=-1$ levels are degenerate even in an electric field. In an electrostatic trap of the kind used by Bethlem *et al.* the trapped states are the weak-field seekers, i.e., those whose Stark energy rises with rising field. These are the $||M_N|,p\rangle = |1,-\rangle$ states in the model. In this paper we will focus exclusively on molecules initially in this state.

The Hamiltonian for collisions between the molecules consists of four terms in this model,

$$\hat{H} = \hat{T} + \hat{H}_{\rm fs} + \hat{H}_{\rm field} + \hat{H}_{\rm dip\text{-}dip}. \tag{1}$$

Here $\hat{T}$ represents the kinetic energy, $\hat{H}_{\rm fs}$ the molecular fine structure including the Λ doubling, and the last two terms are the electric-field interaction and the dipole-dipole interaction between molecules:

$$\hat{H}_{\rm field} = -(\vec{d}_1 + \vec{d}_2)\cdot\vec{\mathcal{E}}, \tag{2}$$

$$\hat{H}_{\rm dip\text{-}dip} = \frac{\vec{d}_1\cdot\vec{d}_2 - 3(\hat{R}\cdot\vec{d}_1)(\hat{R}\cdot\vec{d}_2)}{R^3}, \tag{3}$$

where $\hat{R}$ denotes the orientation of the vector joining the centers of mass of the molecules. Dispersion and exchange potentials are neglected here since they are of secondary importance to dipolar interactions at large R. To avoid problems with the singularity of $1/R^3$ at $R=0$, vanishing boundary conditions are imposed at a cutoff radius $R_0 = 10$ a.u., where the potentials are deep compared to Δ. Thus the model treats only the influence of the long-range dipolar interactions in driving inelastic processes.

In the scattering calculation the molecules are assumed to be identical bosons, so that only even partial waves are relevant. Only the partial waves $L=0$ and $L=2$ are included explicitly, even though in principle all partial waves are coupled together by strong anisotropic interactions. However, the influence of neglected higher-L partial waves can be shown, in the Born approximation, to fall off rapidly with increasing L [9,10]. Cross sections for processes that change molecular channel $|i\rangle$ into channel $|i'\rangle$ are given as in Ref. [11]:

$$\sigma_{i\to i'} = \frac{\pi}{k_i^2}\sum_{LM_L L'M_L'} |\langle i,LM_L|T|i'L'M_L'\rangle|^2, \tag{4}$$

where T is the T matrix for scattering and k_i is the incident wave number. All results, for both elastic and state-changing collisions, will be reported as event rate coefficients,

$$K_{i\to i'} = v_i \sigma_{i\to i'}, \tag{5}$$

where v_i is the incident relative velocity of the collision partners. In this paper we will distinguish two types of rate coefficient: elastic rates $K_{\rm el}$ for which $i=i'$, and loss rates $K_{\rm loss}$ for collisions in which at least one molecule is transformed into a strong-field-seeking state.

The scattering rates can vary significantly depending on the values of the various molecular parameters d, q_Λ, and mass m, as well as the collision energy E. This is illustrated in Fig. 2, which plots the loss rate $K_{\rm loss}$ in zero electric field, over the range of molecular parameters summarized in Table I. In the figure these rates are plotted as a function of the Λ doublet parameter q_Λ, over a range that covers realistic values. The different curves in this figure are the results for different values of d between 0.1 D and 10 D, and values of m between 20 amu and 200 amu; all calculations are performed at a collision energy of $E/k_B = 10^{-6}$ K. The main point illustrated here is that the loss rates span an enormous range, as much as six orders of magnitude even for a fixed value of q_Λ. A second point is that, generically, the rates decrease as q_Λ increases. Thus it appears that a general rule for preserving weak-field seekers is to choose molecules with a large Λ doublet splitting.

A pair of simple semiempirical scaling relations serve to organize the dependence of the rates on the molecular parameters, at least in the zero-field limit. To see this, note first that the ''figure of merit'' for whether the loss rate is suffi-

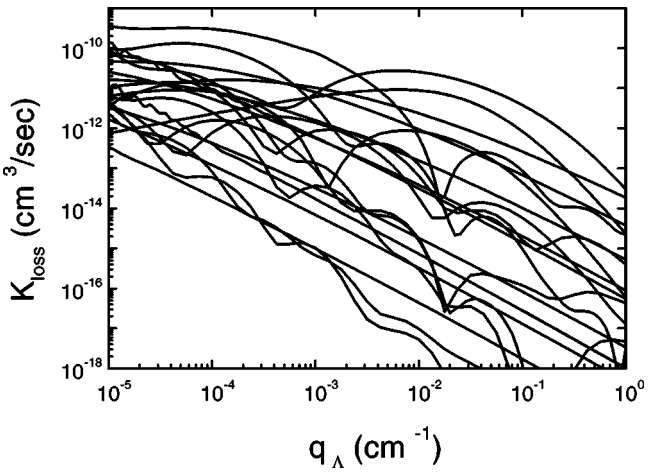

FIG. 2. Electric dipolar relaxation rate constants $K_{\rm loss}$ for collisions of $|M_N,p\rangle=|+1,-\rangle$ molecules, versus the Λ doublet parameter q_Λ. Each curve represents a particular value of dipole moment d and molecular mass m, spanning the ranges indicated in Table I.

ciently small to permit such applications as evaporative cooling is actually the ratio $K_{\rm loss}/K_{\rm el}$ of loss rates to elastic collision rates. Roughly speaking, this ratio must be less than $\sim 10^{-2}$, so that a sufficient number of elastic collisions are able to cool the gas before lossy collisions eject them from the trap [12].

This ratio of lossy and elastic collisions appears to scale roughly with one or the other of a pair of dimensionless quantities, which we will call η_1 and η_2. To motivate the scaling physically, we first present in Fig. 3 a different ''slice'' through the computed results. Here we plot both $K_{\rm loss}$ and the elastic rate $K_{\rm el}$ versus the dipole moment d, for fixed values $q_\Lambda=10^{-3}$ cm^{-1} and $m=20$ amu. Two distinct behaviors are seen: (i) For small values of d the loss rate has generally a high value, then oscillates rapidly while diminishing in value; (ii) for larger values of d the rate instead grows with increasing d and does not oscillate. Examination of the exit channels reveals that these two behaviors arise from distinct physical processes. In case (i) the dominant losses are due to exothermic processes that produce at least one molecule in the parity $p=+1$ state, thus gaining a kinetic energy $\Delta=q_\Lambda N(N+1)$. In case (ii) the dominant losses are instead to molecular states of different angular momentum that are degenerate in energy with, and share the parity of, the incident channel.

We understand the behavior in case (i) according to the Franck-Condon principle. The transition amplitude is proportional to the overlap $\langle\psi_i|\psi_o\rangle$ between incident and outgoing wave functions. The incident channel wave function ψ_i is

TABLE I. The ranges of physical parameters that were explored in the present model.

Quantity	Range
m	20–200 amu
d	0.1–1.0 D
q_Λ	10^{-5}–1.0 cm^{-1}

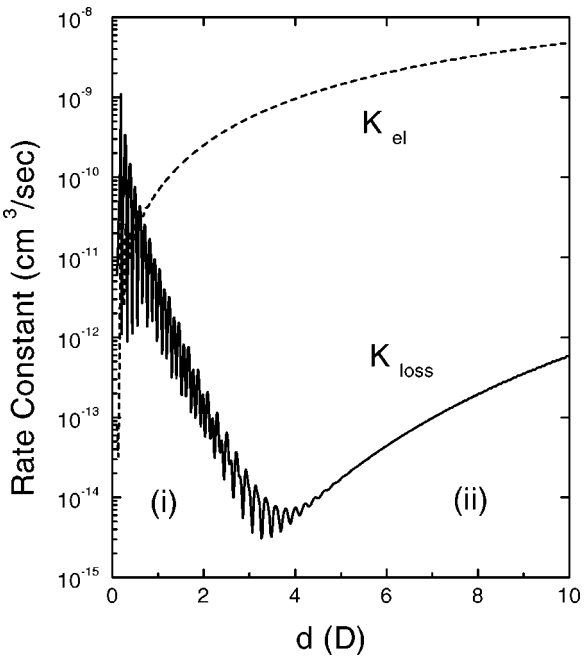

FIG. 3. Example of the variation of the loss rates $K_{\rm loss}$ with the molecular dipole moment d. Shown is the case where $m=20$ amu and $q_\Lambda=10^{-3}$ cm^{-1}. Quite generally, two regions of behavior are observed: (i) The rate oscillates and diminishes with increasing d for low values of d, and (ii) the rate grows with increasing d for large values of d. These behaviors are explained in the text. For comparison the elastic rate constant is also shown (dashed line).

characterized by a large de Broglie wavelength at large R, whereas the outgoing wave function ψ_o is governed by a potential relative to the incident threshold of the form

$$-\frac{C}{R^3}+\frac{\hbar^2L(L+1)}{mR^2}-q_\Lambda N(N+1). \tag{6}$$

Here C is an effective C_3 coefficient for the exit channel. Apart from numerical factors that depend on channel details, its value is $C\sim d^2$. The potential (6) is characterized by a centrifugal barrier of height $B_h=\hbar^6/m^3d^4$, again neglecting numerical factors. The greatest contribution to the Franck-Condon overlap arises from the top of this barrier where the outgoing channel's de Broglie wavelength is greatest. The overlap therefore decreases whenever the top of the barrier decreases in energy, i.e., whenever either q_Λ increases or B_h decreases. We therefore expect $K_{\rm loss}$ to be an *increasing* function of the dimensionless parameter

$$\eta_1=\frac{B_h}{q_\Lambda}=\frac{\hbar^6}{m^3d^4q_\Lambda}. \tag{7}$$

In case (ii), where loss is dominated by transitions to final states degenerate with the incident channel, we argue as follows. Since in this case both molecules have the same parity (both negative, in our model), they are not directly coupled to one another by the dipolar interaction $\hat{H}_{\rm dip\text{-}dip}$ in zero electric field [10]. Their coupling is instead of second order,

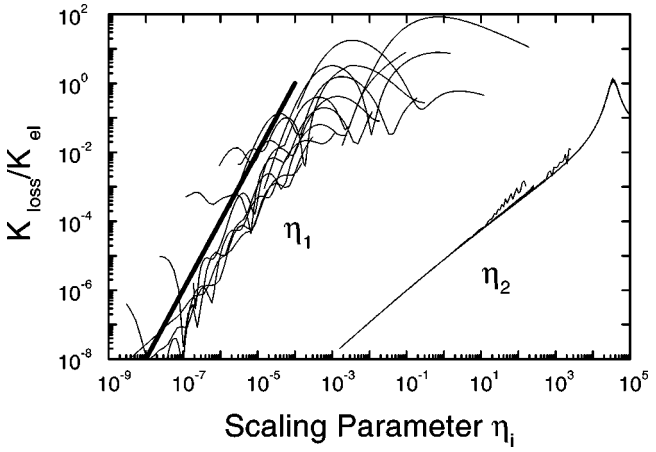

FIG. 4. Loss rates $K_{\rm loss}$ normalized by the corresponding elastic collision rates $K_{\rm el}$ as a function of the molecular scaling parameters η_1 and η_2. The two scalings arise from the two different behaviors in the rates exhibited in Fig. 3, as discussed in the text. The heavy line, which represents $10^8\eta_1^2$, is a guide to the eye.

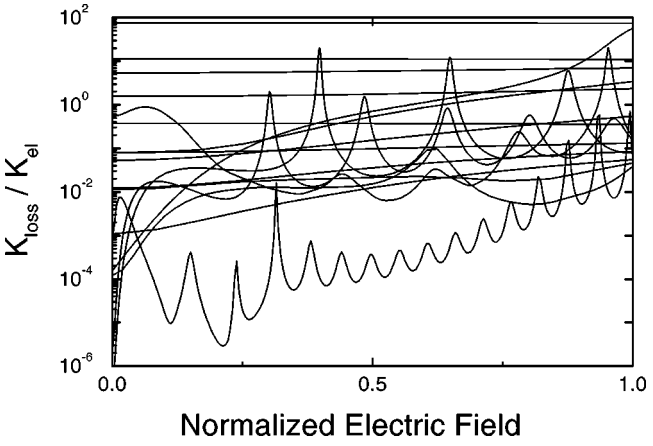

FIG. 5. Electric-field dependence of the ratio $K_{\rm loss}/K_{\rm el}$ for molecules initially in their $|M_N,p\rangle=|+1,-\rangle$ state, in the zero-collision-energy limit. The field $\mathcal{E}$ is rescaled by the critical field $\mathcal{E}_0$ at which the molecular Stark effect becomes linear.

mediated by their direct interaction with channels of opposite parity. The R-dependent interaction term is therefore of the form (again neglecting numerical factors)

$$\frac{1}{q_\Lambda}\left(\frac{d^2}{R^3}\right)^2, \tag{8}$$

where q_Λ is proportional to the energy splitting between states of opposite parity. The equation of motion for the incident wave function ψ_i, including its coupling to an outgoing channel wave function ψ_o, is then

$$-\frac{\hbar^2}{m}\frac{d^2\psi_i}{dR^2}+\frac{\hbar^2L(L+1)}{mR^2}\psi_i+\frac{d^4}{q_\Lambda R^6}\psi_o=E\psi_o. \tag{9}$$

To determine a universal scaling parameter we recast Eq. (9) using the dimensionless length $x=R\sqrt{mE}/\hbar$. Doing so yields the rescaled equation

$$-\frac{d^2\psi_i}{dx^2}+\frac{L(L+1)}{x^2}\psi_i+\frac{\eta_2}{x^6}\psi_o=\psi_i, \tag{10}$$

where the coupling between incident and outgoing channels now resides in the dimensionless quantity

$$\eta_2=\frac{m^3d^4E^2}{\hbar^6q_\Lambda}. \tag{11}$$

We thus expect in this case that $K_{\rm loss}/K_{\rm el}$ will be an increasing function of η_2. Indeed, the presence of E^2 in the definition of η_2 can be regarded as a manifestation of the relative threshold laws for the two rates in this case.

The scaling in these two parameters is illustrated in Fig. 4, which plots $K_{\rm loss}/K_{\rm el}$ versus the appropriate η_i. For the type (ii) processes, which are expected to scale with η_2, the scaling is quite good: this figure shows nine curves with varying physical parameters, all overlapping in the figure. This curve generally follows the trend $K_{\rm loss}/K_{\rm el}\sim 10^{-5}\eta_2^{0.9}$. The type (i) processes do not scale as neatly with η_1, owing partly to their oscillatory behavior. Still, the results are clustered underneath an overall envelope, as suggested by the curve $K_{\rm loss}/K_{\rm el}\sim 10^8\eta_1^2$, which is shown as a heavy line.

This scaling behavior should be viewed as a means of organizing the results of many model calculations, rather than as a means of quantitatively predicting the loss rates for a given molecular species. Nevertheless, the results indicate that there is a fairly large parameter region where the ratio $K_{\rm loss}/K_{\rm el}$ is smaller than 10^{-2}, and hence some molecules may be amenable to evaporative cooling in a static electric dipole trap. For ''small'' dipoles η_1 scaling applies and molecules with large masses are desirable. Vice versa, for ''large'' dipoles η_2 scaling would indicate that small masses and low collision energies favor evaporative cooling. In either event it appears that larger values of q_Λ favor evaporative cooling, all else being equal.

The rates presented in Fig. 4 pertain to the case of collisions in zero electric field. In a realistic trap the field may be small near the trap center, but will necessarily grow in magnitude away from the center, to provide a trapping potential for the weak-field-seeking states. Generally speaking, this field will be of the order of the critical field $\mathcal{E}_0\approx\Delta/d$ where the Stark effect becomes linear. It is therefore vital to know how the loss rates are affected in the presence of a field of this size. The application of the field provides additional channel couplings, since the parity of the molecular states is no longer conserved and the full dipole coupling has been ''activated,'' as discussed above. In this case the loss rates should be larger with a field than without a field.

Figure 5 illustrates that this is indeed the case. This figure plots the figure of merit normalized by the critical field $\mathcal{E}_0$. This scaling enables us to plot many results for many different molecular parameters conveniently on the same graph. Again, many results are possible, but two trends are clear: (i) Those loss rates that started at high values are content to remain at high values; and (ii) Those rates that started at low values are extremely sensitive to the electric field, rising to large values at fields of approximately $\mathcal{E}/\mathcal{E}_0\approx 0.05$. Even

though there are examples where $K_{\mathrm{loss}}/K_{\mathrm{el}}$ remains less than 10^{-2}, as required for evaporative cooling, in general this value is exceeded for electric fields as large as the critical field $\mathcal{E}_0$.

Weak-electric-field-seeking states might be expected to suffer large loss rates. Quantum mechanically this follows from the fact that the large-R Hamiltonian $\hat{H}_{\mathrm{fs}}+\hat{H}_{\mathrm{field}}$ is diagonal in the laboratory frame, while the interaction Hamiltonian $\hat{H}_{\mathrm{dip\text{-}dip}}$ is diagonal in the body frame that joins the centers of mass of the two molecules. The former is stronger at large separations R, while the latter dominates at small R. Molecules that start out in eigenstates of $\hat{H}_{\mathrm{fs}}+\hat{H}_{\mathrm{field}}$ are thus distributed over all the different eigenstates of $\hat{H}_{\mathrm{dip\text{-}dip}}$ during the collision, and reassembled into an assortment of eigenstates of $\hat{H}_{\mathrm{fs}}+\hat{H}_{\mathrm{field}}$ as the molecules separate. Since the asymptotic states are completely deconstructed and reconstructed during this collision, in general it is expected that the probability for inelastic scattering is roughly the same as that for elastic scattering, and that therefore the rates are comparable.

This is of course the same kind of physics that governs spin-exchange collisions in the alkali-metal atoms, which are driven by the competition between hyperfine-plus-magnetic field interactions at large R, and exchange potentials at small R [13]. In the case of alkali-metal atoms it is possible that the short-range phase shifts, from singlet and triplet total electronic spin states, can interfere in such a way as to eliminate probabilities for inelastic processes [14]. For molecules this coincidence seems unlikely, however, since there are many degrees of freedom at short range, all of which would have to contribute nearly identical scattering phase shifts in order to cancel loss rates.

In conclusion, dipolar molecules electrostatically trapped in weak-field-seeking states are generally susceptible to state-changing collisions that can rapidly deplete the trapped gas. In a zero-field region it is possible that the rates for these processes remain quite low for molecules with favorable values of dipole moment, Λ doublet energy, and mass. However, they typically grow dramatically in the presence of the trapping electric field, which effectively turns on the full dipolar coupling at large intermolecular separation. Although this conclusion has been demonstrated using a particular toy model, the physics is quite general and should apply to any polar species. It is therefore recommended that dipolar molecules be trapped in strong-field-seeking states, where inelastic channels are absent at low temperatures. This kind of trapping cannot be achieved in a static trap, but would require a time-varying electric field. Magnetic dipoles in strong-field-seeking states have indeed been confined in such traps, using either time-varying fields [15] or microwave cavities [16]. A more conventional magnetic trap may also be useful, although the influence of the electric dipoles on losses in magnetic traps remains to be explored.

More broadly, an externally applied electric field is seen to have a profound influence on the collision dynamics of ultracold polar molecules. Preliminary results on the unique properties of quantum degenerate gases with dipolar interactions have been reported in the literature [9,17]. More detailed scattering calculations are required to help shape the study of these unusual substances [10].

This work was supported by the National Science Foundation. I acknowledge useful discussions with E. Cornell and C. Greene.

[1] H. L. Bethlem, G. Berden, A. J. van Roij, F. M. H. Crompvoets, and G. Meijer, Phys. Rev. Lett. **84**, 5744 (2000).
[2] H. L. Bethlem, G. Berden, F. M. H. Crompvoets, R. T. Jongma, A. J. A. van Roij, and G. Meijer, Nature (London) **406**, 491 (2000).
[3] A. Fioretti *et al.*, Phys. Rev. Lett. **80**, 4402 (1998); T. Takekoshi, B. M. Patterson, and R. J. Knize, *ibid.* **81**, 5105 (1998); A. N. Nikolov *et al.*, *ibid.* **82**, 703 (1999); R. Wynar *et al.*, Science **287**, 1016 (2000).
[4] J. D. Weinstein *et al.*, Nature (London) **395**, 148 (1998).
[5] K. Mølhave and M. Drewsen, Phys. Rev. A **62**, 011401 (2000).
[6] A. Lagendijk, I. F. Silvera, and B. J. Verhaar, Phys. Rev. B **33**, 626 (1986).
[7] M. Marinescu and L. You, Phys. Rev. Lett. **81**, 4596 (1999).
[8] D. DeMille *et al.*, Phys. Rev. A **61**, 052507 (2000).
[9] S. Yi and L. You, Phys. Rev. A **61**, 041604 (2000).
[10] J. L. Bohn (unpublished).
[11] J. L. Bohn, Phys. Rev. A **62**, 032701 (2000).
[12] J. L. Bohn, Phys. Rev. A **61**, 040702 (2000).
[13] H. T. C. Stoof, J. M. V. A. Koelman, and B. J. Verhaar, Phys. Rev. B **38**, 4688 (1988).
[14] S. J. J. M. F. Kokkelmans, H. M. J. M. Boesten, and B. J. Verhaar, Phys. Rev. A **55**, R1589 (1997); P. S. Julienne, F. H. Mies, E. Tiesinga, and C. J. Williams, Phys. Rev. Lett. **78**, 1880 (1997); J. P. Burke, Jr., J. L. Bohn, B. D. Esry, and C. H. Greene, Phys. Rev. A **55**, R2511 (1997).
[15] E. A. Cornell, C. Monroe, and C. E. Wieman, Phys. Rev. Lett. **67**, 2439 (1991).
[16] R. J. C. Spreeuw *et al.*, Phys. Rev. Lett. **72**, 3162 (1994).
[17] K. Góral, K. Rzążewski, and T. Pfau, Phys. Rev. A **61**, 051601(R) (2000).